

Control of Polymer Molecular Weight Using Near Infrared Spectroscopy

Nida Sheibat Othman and Gilles F  votte

LAGEP-Universit   Lyon I/CNRS-ESCPE Lyon, B  t 308, 43 Blvd. du 11 Nov. 1918, 69622 Villeurbanne Cedex, France

Dominique Peycelon, Jean-Bernard Egraz, and Jean-Marc Suau

Coatex ZI Lyon Nord, 69727 Genay, France

Near Infrared spectroscopy is used to control a polymerization reactor in order to produce solution polymers with well-defined molecular weight. A model for the monitoring of both the average polymer molecular weight, and the concentration of monomer in the reactor is developed with the partial least-squares calibration technique applied to the NIR spectra. On the basis of a process model, a nonlinear input–output linearizing geometric approach is then applied to control the polymer molecular weight by manipulating the inlet flow rate of the monomer. The control strategy is then validated on-line during the solution polymerization of acrylic acid in an industrial pilot scale reactor.

   2004 American Institute of Chemical Engineers *AIChE J.* 50: 654–664, 2004

Keywords: control, polymerization, online estimation, near infrared, molecular weight, process control, polymer properties

Introduction

Polymer molecular weight distribution (MWD) is an important industrial output control variable for many applications of polymer products. The MWD is a fundamental polymer property that directly influences many of the characteristics of the product, such as its mechanical properties. Maintaining the instantaneous molecular weight (MW) constant during the polymerization process allows narrowing the final cumulative MWD, which influences stress–strain properties, stress crack resistance, impact resistance, and thermal properties of many polymer systems (Martin et al., 1972). The weight average MW influences also the melt and concentrated solution viscosity. Therefore, developing strategies for MW and MWD monitoring and control is an important industrial issue.

The main difficulty in controlling the MWD is the lack of on-line sensors to monitor the process. The techniques mostly used for characterizing polydispersed MWD of polymers is size exclusion chromatography (SEC), or gel permeation chro-

matography (GPC). The drawbacks of on-line SEC are, however, the delay of the analysis and the maintenance of the columns, leading to significant difficulties in real-time control. Furthermore, SEC does not give the instantaneous MW value needed in the control loop, but a delayed mean value of the MW. For these reasons, in addition to on-line measurements, as far as polymer quality control is concerned, an efficient control loop should be based on a process model, and an estimator of the instantaneous MW.

The values of the weight average MW and of the MWD profile depend on the choice of the operating conditions, in particular the reaction temperature and the concentrations of monomer, initiator, and chain transfer agent. In order to control MW, the manipulation of the reaction temperature during the operation can be efficient in batch and isothermal operations as proposed by Crowley and Choi (1998). In semi-batch reactions, controlling the MW is more usually done by manipulating the ratio of monomer to initiator and chain transfer agent, which allows us at the same time to minimize the operation time. The combined control of temperature and concentration of additives has been examined by Louie and Soong (1985) and Ellis et al. (1994). Ellis et al. (1994) proposed an extended Kalman filter to estimate the entire MWD, based on measurements of mono-

Correspondence concerning this article should be addressed to N. Sheibat Othman at nida.othman@lagep.cpe.fr.

mer conversion, obtained by on-line densimetry and periodic time-delayed measurements of MWD from on-line SEC.

With the feeding rates of the reagents to control the MW, it becomes particularly interesting when the reaction is very exothermic, which is the case of many polymerization reactions. In this case, the temperature profile cannot be manipulated to control the MW. Therefore, the case in general, the MW is controlled by manipulating the concentrations of monomer, chain transfer agent, and initiator (Adebekun and Schork, 1989; Dimitratos et al., 1989; Congalidis et al., 1989; Kozub and MacGregor, 1992; Clay and Gilbert 1995; Ghielmi, 1998; Florenzano et al., 1998). Echevarria et al. (1998) presented a control strategy of MWD for styrene emulsion polymerization. On-line gas chromatography was used to measure the amount of unreacted monomer and chain transfer agent. The control strategy includes a nonlinear model-based controller and state estimation, based on a nonlinear optimization technique.

The aim of this work is to produce solution polymers with well-defined MW, with on-line near infrared (NIR) spectroscopy. For this purpose, we investigate an industrial process where the end-use properties of the product are mainly determined by the polymer MWD.

With NIR spectroscopy to monitor polymerization processes offers several advantages. First, the fiber optic inserted in an existing reactor is directly in contact with the reaction medium, which ensures rapid measurements without requiring any sample preparation. Fiber optics allows the spectrometer to be placed far away from the reactor and, thus, ensures rapid and precise data transmission. Furthermore, a set of characteristics of the sample can be evaluated from the same spectrum by developing calibration models that can be transferred to other instruments.

Most of the applications of NIR spectroscopy in polymerization processes deal with the on-line monitoring of the monomer concentration (Long et al., 1993; Chabot et al., 2000; Aldridge et al., 1993). NIR spectroscopy can also be employed to estimate some physical properties. Gossen et al. (1993) used NIR spectroscopy to estimate the concentration of styrene and the particle size in an emulsion polymerization. Santos et al. (1998) used the NIR to estimate the particle size in suspension polymerizations of styrene. The authors used PLS and Neuron nets to correlate the measured absorbances with the particle size. Their results allowed the authors (Santos et al., 2000) to develop a policy to control the particle size in a batch process.

The process studied in this article is a semicontinuous solution free radical polymerization of acrylic acid (AA). After a presentation of the process setup, a calibration model based on the NIR spectrum is developed to estimate the concentrations of monomer and polymer in the reactor, and the polymer average molecular weight. For the design of the MW control system, a deterministic process model must be available. Development and identification of the model are presented in this article. The parameters involved in the model are estimated from experimental data with a high gain observer. The model describes the effects of the chain transfer agent (CTA), initiator, and monomer concentrations on the kinetics, and on the MW. A nonlinear estimator is developed to provide an estimate of the reaction rate needed in the control loop. Finally, a nonlinear input-output linearizing controller is implemented to control the instantaneous MW. The control strategy calculates

in-line the feed rate of monomer needed to obtain the desired MW.

Experimental setup

The semicontinuous solution free radical polymerization of AA is carried out in a 30 L jacketed well-mixed reactor, equipped with an internal reflux condenser. The stirrer is equipped with a Rushton turbine, the stirring rate being 150 rpm. Four volumetric pumps are used to feed the reactor with initiators, monomer, and solvent. Four flowmeters allow the measurement of the flow rate of the pumps. The flow rate set point of additives can be manipulated on-line.

The main temperatures of the plant are measured with Pt100- Ω probes. Measurements of temperatures and flow rates are acquired and stored on a computer. The NIR transmission probe is immersed in the reactor, and is connected through fiber optics to a FOSS NIRSystems® industrial spectrometer. The spectral data are acquired and processed by a second computer. The state observer and the control law described below are computed and applied with the same computer. Both computers are connected in order to exchange data.

The reactor is initially charged with all the desired amount of solvent (isopropyl alcohol), which plays the role of CTA during the polymerization, water, and a small amount of initiator. This charge is then heated to 80°C through the jacket. Monomer and initiators are then introduced at fixed flow rates. Radicals are produced by a redox reaction. During the reaction, the condenser maintains the reactor temperature at 80°C by condensing the evaporated solvent. The final process solids content attains 45% in about 2 h, which corresponds to the “usual” processing time. When the total amount of monomer is added the reaction continues to consume the residual monomer. Gas chromatographic measurements have shown that the amount of solvent remains almost constant during the reaction. A negligible amount of solvent is consumed by the transfer reactions and, therefore, the amount of solvent can be considered constant during the reaction in the process model.

During model development, samples are withdrawn from the reaction medium and analyzed for residual amount of acrylic acid by high pressure liquid chromatography (HPLC), and for molecular-weight distribution by gel permeation chromatography (GPC). A GPC comprising a 515 Waters pump, one or two Ultrahydrogel Linear 7.8 mm 30 cm columns (mixed-bed column with the pore size ranging from 120 to 2,000 Å²), were used with a guard precolumn, and a 410 Waters refractometer. Elution was performed at 60°C (0.5 mL/min) with an aqueous buffer (NaHCO₃ 0.05M, NaNO₃ 0.1M, triethanolamine 0.02M, Na₃N 0.03%). Calibration was relative to polyacrylic acid standards. GPC samples were neutralized with sodium hydroxide before injection in the GPC.

Calibration of the NIR measurements

The quality of the NIR analysis depends on the impact of the required properties in the NIR region, and on the precision of the off-line measurements used for the calibration of the spectrum. The performance of the instrument, and the mathematical treatment of the acquired spectra also influence the NIR analysis, and have to be adapted to the process in question.

Multivariable calibration methods, such as partial least

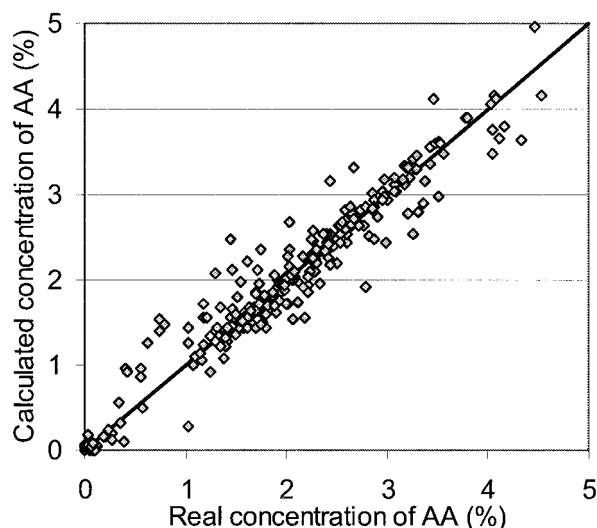


Figure 1. NIR Calibration for the estimation of the concentration of AA in the reactor.

squares (PLS), and Multiple Linear Regression (MLR), are necessary to calibrate the spectra. In this work, a PLS technique was used to develop calibration models of the monomer and polymer concentrations in the reactor, and the average polymer molecular weight. The input data used to calibrate the NIR spectrometer were obtained by HPLC for the monomer concentration, and with GPC for the polymer MW measurements.

In order to obtain a good model, the calibration set must contain data resulting from varied experimental conditions. The concentration of polymer varies from 0 to 45% during the reaction, which gives a precise evaluation of the solids content in this region. In order to vary the concentration of monomer during the reaction, experiments with different monomer and initiator flow rates were carried out. In the calibration of the molecular weight, the experiments were realized in a way that allows us to decouple the molecular weight evolution from the concentrations of reactants. This can be done by maintaining the same molecular weight, whereas varying the amount of monomer. In this case, the concentration of solvent can be used to vary the molecular weight. Thus, the concentration of monomer was used to vary the molecular weight, and the concentration of solvent was maintained constant. One must be aware that even in this case we might have an implicit estimation of the molecular weight from the concentration of reactants, and not a real sensitivity of the NIR spectrum on the variation of the chain length.

Figures 1, 3, and 5 show the results of calibration of the concentration of monomer and polymer, and the number-average molecular weight with the PLS algorithm. For the two measurements of concentration the calibration was based on 290 data points. The calibration resulted in 5 and 6 factors for the monomer and the polymer concentrations, respectively. The calibration errors are 2,500 ppm and 1.55%, the validation errors are 2,700 ppm and 1.65%, and the determination coefficients $R^2 = 0.97$, and 0.987 for the monomer and the polymer concentrations, respectively. The calibration of the average number molecular weight is based on 480 measured data. The model resulted in 10 factors, with a calibration error of 179 g/mol, a validation error of 229 g/mol, and $R^2=0.80$.

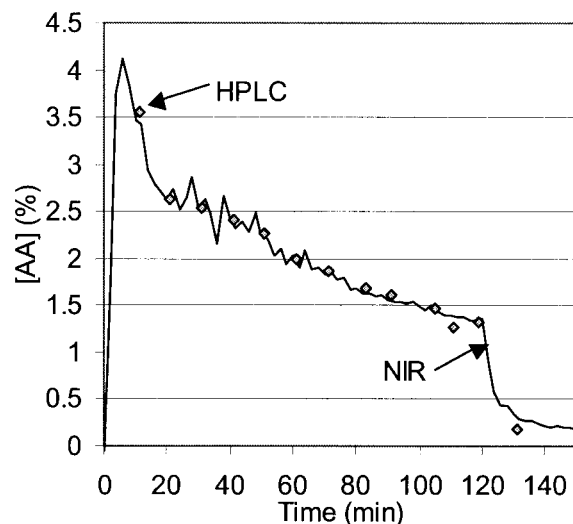


Figure 2. Validation of the NIR calibration for the in-line estimation of the concentration of AA.

Experimental validations of the NIR measurements during a semicontinuous polymerization of AA are shown in Figures 2, 4 and 6. We observe a good correlation between the predicted and measured values. The model of the monomer concentration is inaccurate only at very small amounts of monomer ($<1,700$ ppm). The model of the molecular weight is inaccurate when there is a small amount of polymer in the reactor. Therefore, the first estimates of the molecular weight must be considered with vigilance.

Process model

The monomer mass balance of a semicontinuous polymerization reaction is given by the following equation

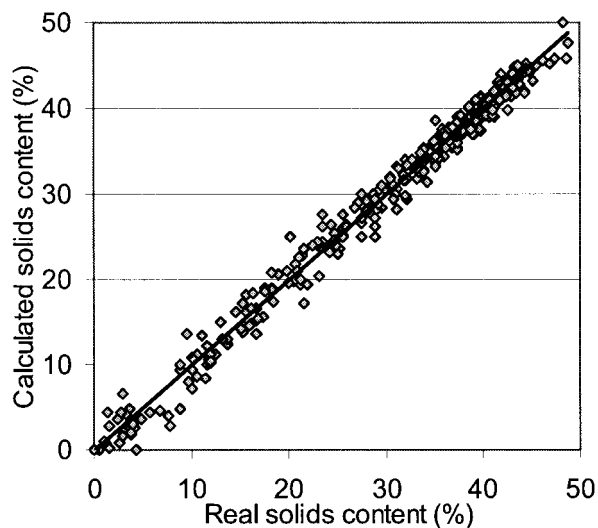


Figure 3. NIR Calibration for the estimation of the polymer solids content.

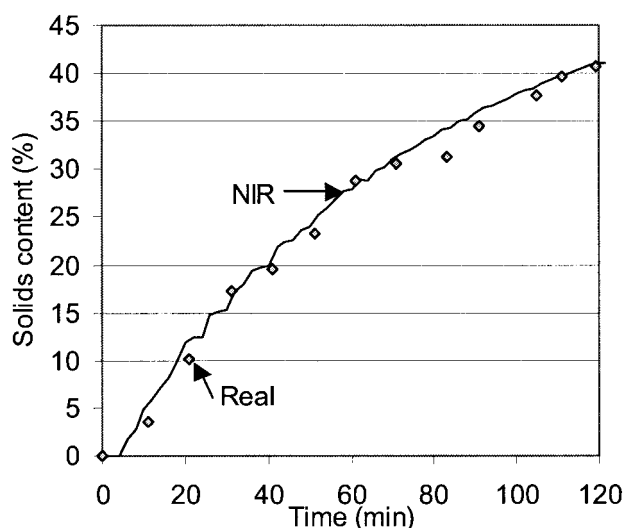


Figure 4. Validation of the NIR calibration for the in-line estimation of the solids content.

$$\frac{dN_{AA}}{dt} = Q_{AA}^{in} - R_p = Q_{AA}^{in} - \underbrace{k_p[R^*]N_{AA}}_{R_p} \quad (1)$$

Significant transfer to solvent (isopropyl alcohol) occurs which limits the chain growth. The rate of transfer to solvent is, therefore, important to determine the polymer molecular weight, in general it does not affect the propagation rate. The mass balance of the solvent is given by the following system

$$\frac{dN_s}{dt} = Q_s^{in} - \underbrace{k_f[R^*]N_s}_{R_f} \quad (2)$$

The degree of polymerization D_p is the average number of molecules of monomer in the polymer chains. This is equal to

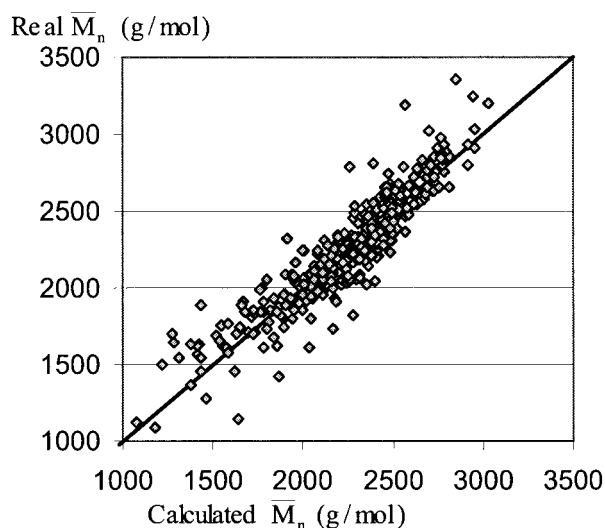


Figure 5. NIR Calibration for the estimation of the number-average molecular weight.

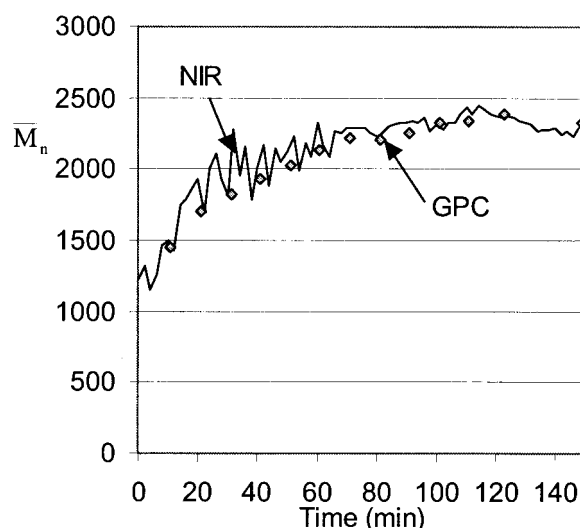


Figure 6. Validation of the NIR model estimating the molecular weight.

the rate of polymerization divided by the rate of chain stoppage by termination, or transfer to solvent

$$D_p = \frac{R_p}{R_t + R_f} = \frac{k_p[R^*]N_{AA}/V}{k_t[R^*]^2V + k_f[R^*]N_s/V} \quad (3)$$

The polydispersity of the polymer in the process under investigation is not very large, and one can assume that there is no transfer to polymer. Advanced analyses have shown that termination through disproportionation takes place, whereas combination is negligible. Therefore, the degree of polymerization is equal to the number of units in the polymer chain. The number-average molecular weight can therefore be calculated from the degree of polymerization as follows

$$M_n = MW_{AA} \times D_p \quad (4)$$

The parameters k_p , k_t and k_f are not known for this system. It is well known that the propagation rate constant of acrylic acid is difficult to predict as it depends on the pH variations during the reaction. Kabanov et al. (1973) have shown that the reaction rate decreases between pH 1 to 6, and increases again between pH 7 to 11. The authors deduced that the change in the reaction rate was because of a change in k_p , since k_t does not depend on the pH. Figure 7 shows that the pH decreases slightly during the reaction in our process. In this pH region, the propagation rate constant is of the order of 1×10^8 cm³/mol/s, according to Kabanov.

Several experiments were performed with different experimental conditions in order to investigate more deeply the process behavior, and to estimate the unknown parameters of the process model. First of all, the initiator concentration was varied. As expected, these experiments showed that the concentration of monomer and the polymer molecular weight are sensitive to changes in the flow rate of the initiator, as shown in Figures 8 and 9. Increasing the flow rate of initiator decreases both the amount of residual monomer and the number-average molecular weight. Figure 10 shows, however, that the

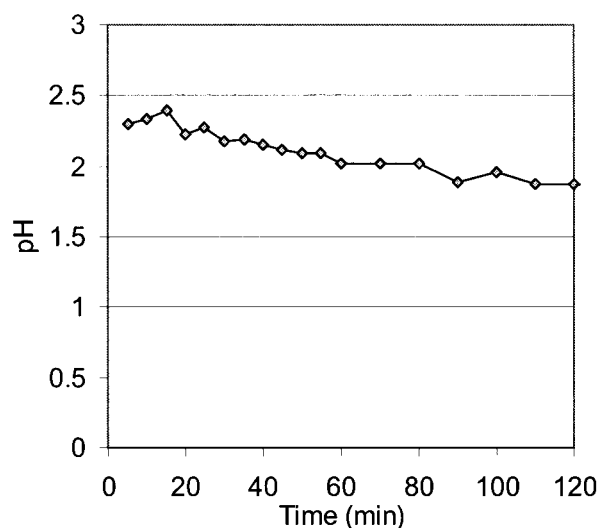


Figure 7. Evolution of pH during a semicontinuous process.

ratio of monomer to \bar{M}_n remained almost constant. This means that the chain lengths are mainly determined by transfer to solvent mechanisms, and that termination reactions can be neglected. As expected, the polydispersity increases with \bar{M}_n as shown in Figure 11.

The influence of the concentration of solvent on the reaction kinetics was also studied. These experimental results show that \bar{M}_n is inversely proportional to the concentration of solvent (Fig. 12), whereas the concentration of AA remains constant (Figure 13). This confirms that the polymer molecular weight is solely controlled by transfer to solvent. Therefore, Eq. 3 reduces to

$$D_p = \frac{k_p N_{AA}}{k_f N_s} \quad (5)$$

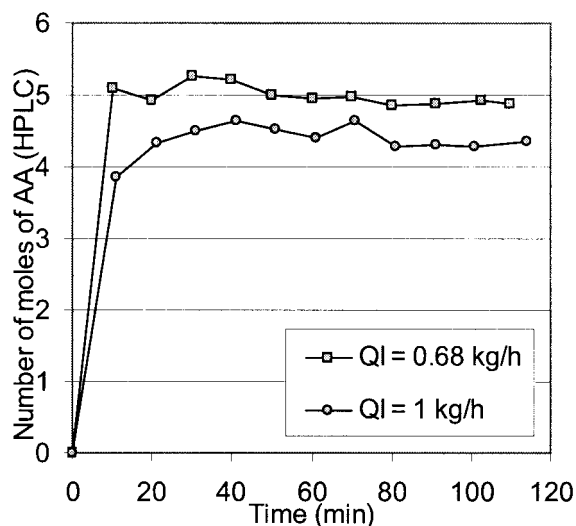


Figure 8. Effect of the initiator flow rate on N_{AA} .

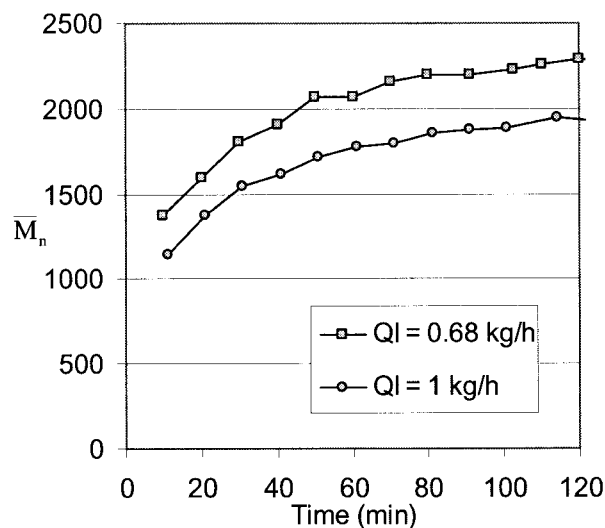


Figure 9 Effect of the initiator flow rate on \bar{M}_n .

Under these conditions, if one applies the stationary state hypothesis for the active chains, the balances of these chains allows us to calculate the moments of the chain-length distribution of active chains as follows

$$\lambda_0 = [R^*] \quad \lambda_1 = \frac{k_p \lambda_0 N_{AA}}{k_f N_s} \quad \lambda_2 = \left(1 + \frac{2\lambda_1}{\lambda_0}\right) \lambda_1 \quad (6)$$

The material balances of the moments of the chain-length distribution of inactive polymer give

$$\frac{d\mu_0}{dt} = k_f \frac{N_s}{V} \lambda_0 \quad \frac{d\mu_1}{dt} = k_f \frac{N_s}{V} \lambda_1 \quad \frac{d\mu_2}{dt} = k_f \frac{N_s}{V} \lambda_2 \quad (7)$$

The cumulative number and weight-average molecular weights can be calculated from the moments of the chain-length distribution as follows

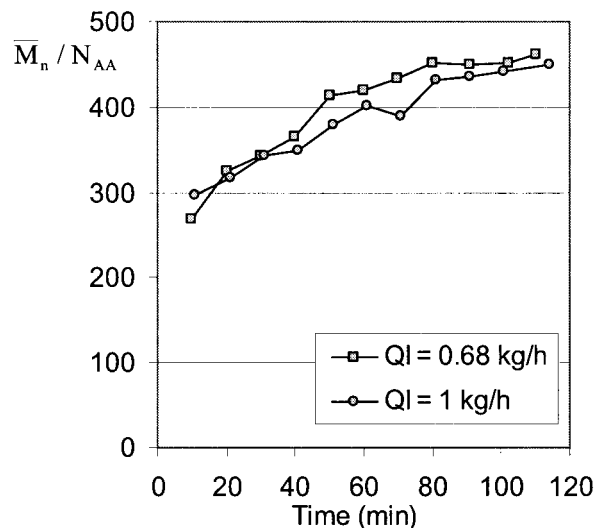


Figure 10. Effect of the initiator flow rate on \bar{M}_n/N_{AA} .

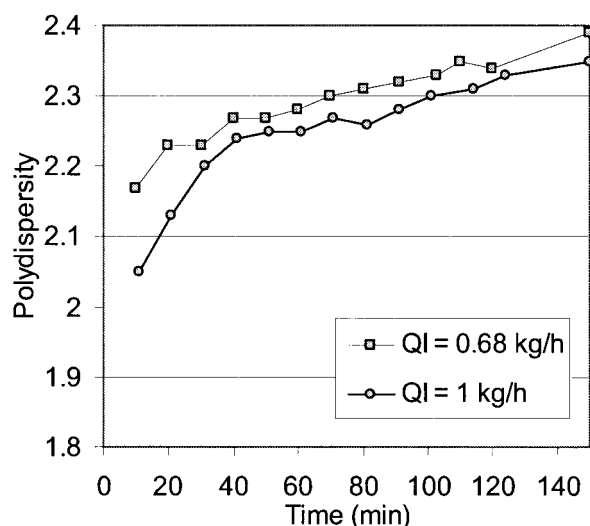


Figure 11. Effect of the initiator flow rate on the molecular polydispersity.

$$\bar{M}_n = \frac{\mu_1}{\mu_0} MW_{AA} \quad \bar{M}_w = \frac{\mu_2}{\mu_1} MW_{AA} \quad (8)$$

It is important to point out that realizing that the experiments with a fixed monomer to solvent ratio in the feed does not guarantee a reproducible production and, therefore, does not allow us to control \bar{M}_n . The main reason that makes this technique fail is that at the beginning of the reaction, a certain amount of monomer is accumulated until the reaction starts because of the inhibition phenomena, which significantly affects \bar{M}_n . Experiments with identical operating conditions might have different behaviors, as illustrated by Figures 14 and 15. These figures show that during two identical experiments (that is, 116 and 120) the concentration of monomer and, therefore, the polymer molecular weight evolve differently. For these reasons, the on-line measurement of the concentration of

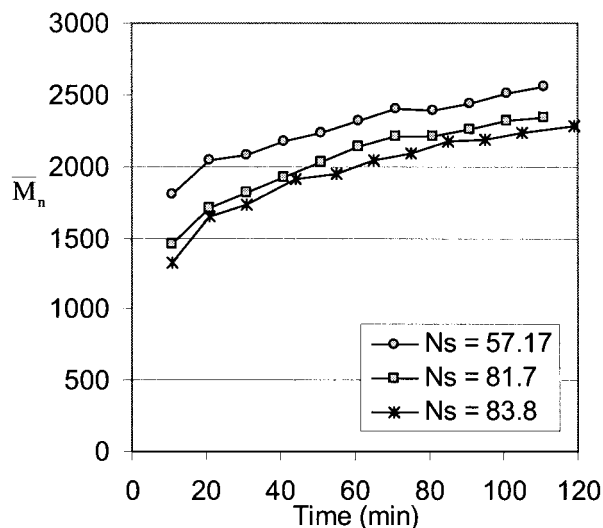


Figure 12. Effect of the solvent concentration on \bar{M}_n .

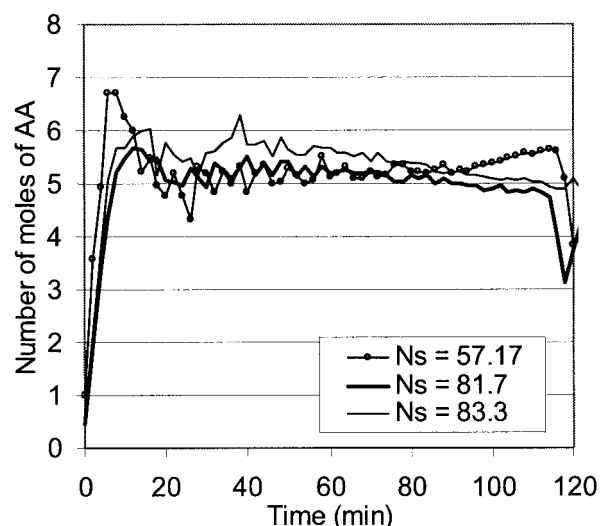


Figure 13. Effect of the solvent concentration on N_{AA} .

monomer is necessary to control the polymer molecular weight.

Estimation of the reaction rate

With the NIR in-line measurement of the monomer concentration the reaction rate can be estimated. Thus, we consider the following state space representation where ϵ represents the unknown dynamic of R_p (mol/s)

$$\begin{bmatrix} \dot{N}_{AA} \\ \dot{R}_p \end{bmatrix} = \begin{bmatrix} Q_{AA}^{in} \\ 0 \end{bmatrix} + \underbrace{\begin{bmatrix} 0 & -1 \\ 0 & 0 \end{bmatrix}}_A \begin{bmatrix} N_{AA} \\ R_p \end{bmatrix} + \begin{bmatrix} 0 \\ \epsilon \end{bmatrix} \quad (9)$$

Performing a change of coordinates allows one to put the system under a canonical form of observability and, therefore, to apply a high gain observer to estimate R_p (see Farza et al., 1997)

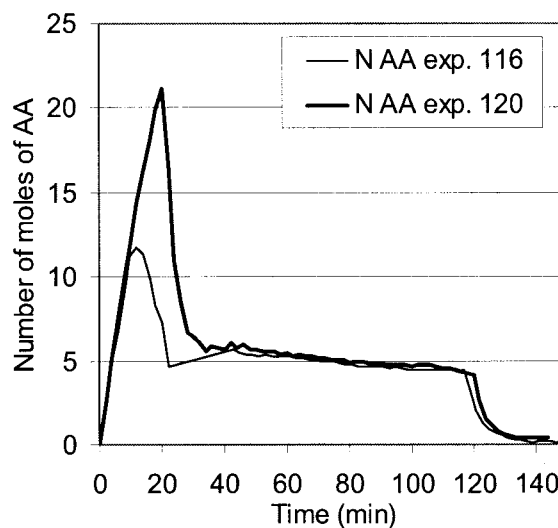


Figure 14. Effect of inhibition on the concentration of monomer.

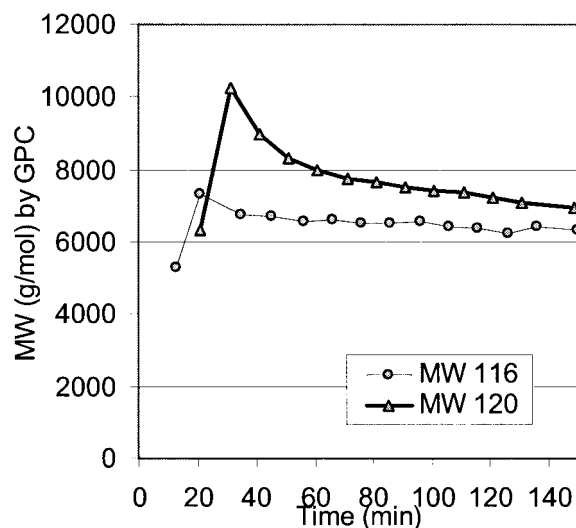


Figure 15. Effect of inhibition on \bar{M}_n .

$$\begin{bmatrix} \dot{\hat{N}}_{AA} \\ \dot{\hat{R}}_p \end{bmatrix} = \begin{bmatrix} Q_{AA}^{in} \\ 0 \end{bmatrix} + \underbrace{\begin{bmatrix} 0 & -1 \\ 0 & 0 \end{bmatrix}}_A \begin{bmatrix} N_{AA} \\ R_p \end{bmatrix} - \begin{bmatrix} 2\theta \\ \theta^2 \end{bmatrix} (\hat{N}_{AA} - N_{AA}) \quad (10)$$

The rate of convergence of the observer is determined by the positive parameter θ .

Estimation results obtained during a semicontinuous reaction are shown in Figure 16. We noticed that when no monomer accumulation takes place during the reaction, the reaction rate is thus equal to the flow rate of the monomer.

Estimation of the instantaneous MW and k_f

Estimating the instantaneous molecular weight requires the knowledge of k_p/k_f . In the previous experiments, it was observed that the number of moles of monomer remains constant during the semicontinuous polymerization reaction, whereas \bar{M}_n increases with time (see, for example, Figures 12 and 13). According to Eq. 5, this means that the ratio k_p/k_f increases with time. This increase might be because of the gel effect that affects the mobility of polymer chains. The kinetic parameters k_f and k_p might depend on diffusive limitations, which increase with increasing solids content (45%), suggested by Clay and Gilbert (1995), for pseudobulk polymerizations.

However, since such complex variations of the kinetic constants are not well understood and are outside the scope of this work, a method for estimating the ratio of k_f/k_p was developed with in-line NIR – or off-line GPC – measurements of the number-average molecular weight. The distinct values of these two parameters are not required in the control scheme.

It can easily be seen that the ratio k_f/k_p is observable from the first moment of the inactive chains if the reaction rate is known. The reaction rate can be computed with the observer developed above (Eq. 10). The following augmented system uses the first moment of the inactive chains, and assumes that k_f/k_p varies with an unknown dynamic ε'

$$\underbrace{\begin{bmatrix} d\mu_0/dt \\ d(k_f/k_p)/dt \end{bmatrix}}_{dx/dt} = \underbrace{\begin{bmatrix} (k_f/k_p) N_s R_p / (V \cdot N_{AA}) \\ \varepsilon' \end{bmatrix}}_f \quad (11)$$

$$y = \bar{M}_n = \frac{\mu_1}{\mu_0} MW_{AA}$$

where y is the process output, measured with NIR or GPC. In order to develop an observer of k_f/k_p , the following change of coordinates is applied to the system

$$T = \begin{bmatrix} y \\ L_f y \end{bmatrix} = \begin{bmatrix} \frac{\mu_1}{\mu_0} MW_{AA} \\ -\frac{\mu_1}{\mu_0^2} MW_{AA} R_f \end{bmatrix} \quad (12)$$

where R_f is the rate of transfer to solvent (mol/cm³/s), and $L_f y$ is the Lie derivative of y with respect to f . The variation of T with time is an observable system with respect to y and to $L_f y$, since it can be written under the form

$$\dot{T} = \underbrace{\begin{bmatrix} 0 & 1 \\ 0 & 0 \end{bmatrix}}_A T + \begin{bmatrix} 0 \\ \varphi(T) \end{bmatrix} \quad (13)$$

A high gain nonlinear observer can now be constructed to estimate the states T . In order to obtain an exponential observer of the original states μ_0 and k_f , we apply the inverse of the change of coordinates performed in Eq. 12 as follows

$$\begin{bmatrix} \frac{d\hat{\mu}_0}{dt} \\ \frac{d}{dt} \left(\frac{\hat{k}_f}{\hat{k}_p} \right) \end{bmatrix} = \begin{bmatrix} \left(\frac{\hat{k}_f}{\hat{k}_p} \right) \frac{N_s}{N_{AA}} \frac{R_p}{V} \\ 0 \end{bmatrix} - \left(\frac{\partial T}{\partial \hat{x}_i} \right)^{-1} S_\theta^{-1} C^T (\hat{y} - y) \quad (14)$$

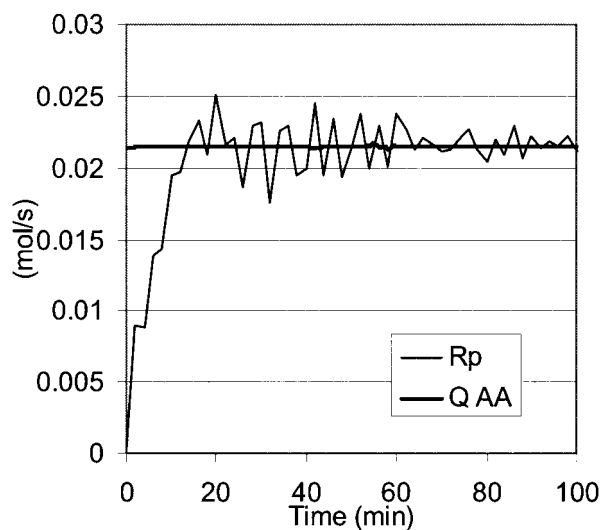


Figure 16. Estimation of the reaction rate with a high gain observer.

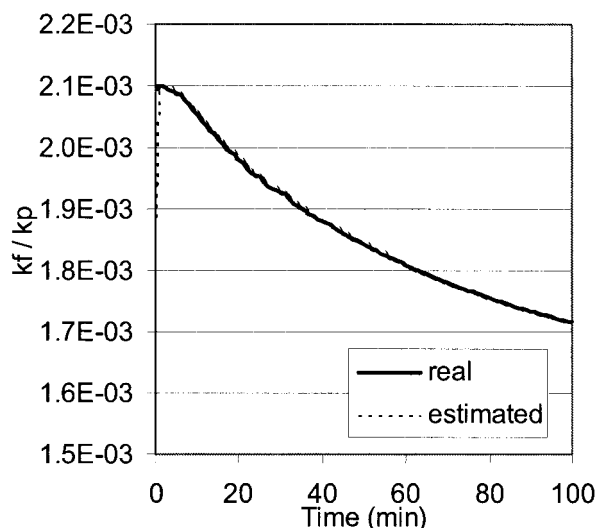


Figure 17. Simulation of the observer of k_f/k_p with 10% error in the initial value and $\theta=0.01$.

where $C=[1 \ 0]$ and S_θ is the unique symmetric positive definite matrix satisfying the algebraic Lyapunov equation

$$\theta S_\theta + A^T S_\theta + S_\theta A - C^T C = 0 \quad (15)$$

which gives

$$S_\theta = \begin{bmatrix} \frac{1}{\theta} & -\frac{1}{\theta^2} \\ -\frac{1}{\theta^2} & \frac{2}{\theta^3} \end{bmatrix} \quad (16)$$

Figure 17 presents simulation results validating the observer. The ratio k_f/k_p was initialized with a 10% error between the observer and the process. It can be seen from this simulation that the observed value converges immediately to the true one. NIR measurements were then used to estimate the real ratio k_f/k_p . As expected, Figure 18 shows that k_f/k_p decreases with increasing solids content. The observed decrease of the ratio k_f/k_p is rather difficult to interpret. A significant transfer to solvent might occur under the diluted conditions taking place at the beginning of the reaction. With the increasing weight fraction of polymer, transfer, and propagation become diffusion-controlled. It is likely that many complex and competitive phenomena are involved here, which results in a global effect of the decrease of k_f/k_p . Moreover, the estimation might be attached with error because of neglecting chain termination in the process model. It is plausible, chain termination cannot be neglected at the very beginning of the reaction when many radicals are present in the reactor. For these reasons, the two kinetic parameters should be regarded simply as tuning model parameters necessary for the control purpose.

It was noticed that under similar conditions, k_f/k_p presents the same profile as a function of the solids content. Therefore, a linear correlation could be developed to estimate k_f/k_p as a function of solids content that is easier to measure than the molecular weight in most processes.

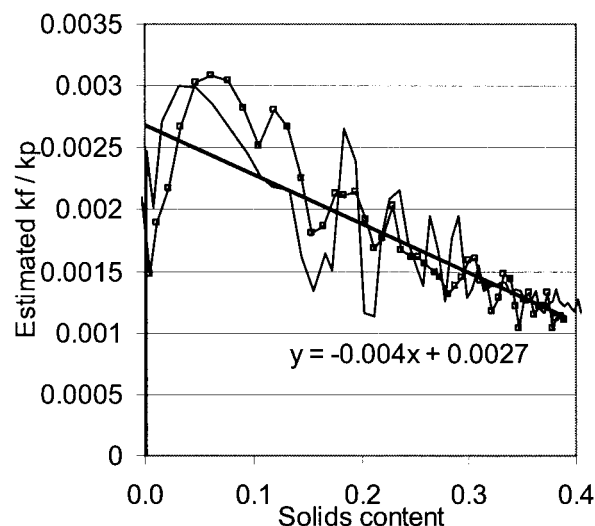


Figure 18. Estimation of k_f/k_p during the reaction.

The estimated value of k_f/k_p is then used to estimate the instantaneous molecular weight required in the computation of the control law (Eq. 5). The estimation results are illustrated in Figure 19, with k_f/k_p values obtained first with the observer, and second with a correlation established with the solids content. One can notice that the values of M_n obtained by both ways are very adjacent. Therefore, it turns out that the correlation can be used on-line to estimate the instantaneous molecular weight. It also appears that the instantaneous molecular weight reaches 4,000 g/mol at the end of the reaction, whereas the maximum average molecular weight does not exceed 2,500 g/mol. The small amount of polymer produced with high molecular weights at the end of the reaction does not significantly influence the average molecular weight.

A nonlinear strategy for controlling the MW

Controlling MW can be done by manipulating the concentration of monomer, initiator, or solvent in the reactor or the

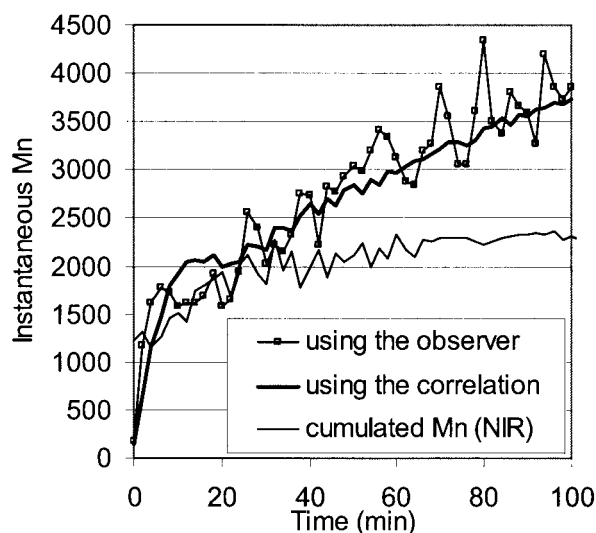


Figure 19. Estimation of M_n with the observer, and the correlation with the solids content.

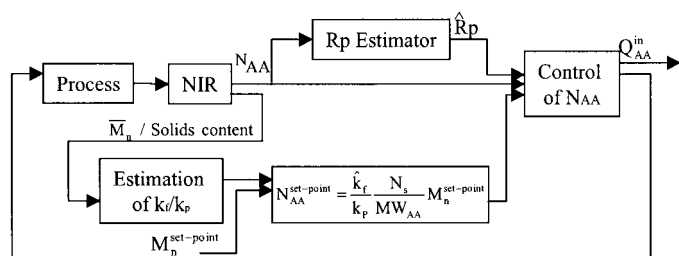


Figure 20. Control scheme for semicontinuous polymerization of AA.

reaction temperature. However, some of the process conditions cannot be manipulated easily in the process under investigation. First it is reasonable to avoid with the reaction temperature to control MW because the solvent might evaporate at high temperatures, and the initiator has poor efficiency at low temperatures. Second, the concentration of solvent in the reactor cannot be used to control the molecular weight because it must remain constant so as to maintain good diffusion and heat transfer features of the process. Finally, the concentration of initiator is not a suitable variable to control MW, as it is important to maintain enough radicals in the reactor in order to ensure a sufficient reaction rate, in particular at the beginning of the reaction. Furthermore, chain length is limited by transfer to solvent phenomena (monomer to solvent ratio), and not by termination. Manipulating the concentration of radicals in the reactor affects the MW mainly because it affects the concentration of residual monomer, which modifies the ratio of monomer to solvent. Consequently, it appears that an efficient strategy aiming at controlling MW lies in the direct manipulation of the concentration of monomer through manipulating the inlet flow rate of monomer. It is obvious that controlling the concentration of acrylic acid in the reactor is also essential to maximize the process productivity by decreasing the reaction time, while ensuring the process thermal safety. Because the polymerization of AA is very exothermic and rapid, the amount of monomer in the reactor must be calculated in a way that the cooling system is able to evacuate the heat produced by the polymerization, and also to maintain the desired reaction temperature.

The concentration of monomer is measured on-line by the NIR spectrometer, and, thus, can be controlled by manipulating the flow rate of monomer as given by the following equation

$$\begin{aligned} N_{AA} &= Q_{AA}^{\text{in}} - R_p \\ y &= N_{AA} \end{aligned} \quad (17)$$

We notice that controlling N_{AA} requires the estimation of R_p , which is computed with the high gain observer (Eq. 10). Controlling the polymer MW requires the estimation of k_f/k_p that is obtained with the second nonlinear observer (Eq. 14). In-line measurements of the concentration of monomer, and either the concentration of polymer or the cumulated molecular weight are required to estimate R_p and the instantaneous molecular weight as shown in Figure 20.

As for linear systems, the relative order of nonlinear systems can be obtained by calculating the derivative of the output. The relative order is the smallest order of derivative that depends

explicitly on the input (Q_{AA}). For Eq. 17, the relative order is equal to one. A geometric nonlinear input/output linearizing control can then be constructed as shown below

$$Q_{AA}^{\text{in}} = R_p + \kappa_p (\underbrace{N_{AA}^{\text{set-point}} - N_{AA}}_{\varepsilon = \text{error}}) + \tau'_t (N_{AA}^{\text{set-point}} - N_{AA}) dt \quad (18)$$

where the set point is calculated by the following equation

$$N_{AA}^{\text{set-point}} = \left(\frac{k_f}{k_p} \right) \frac{N_s}{MW_{AA}} MW^{\text{set-point}} \quad (19)$$

Experimental validation of the control strategy

The industrial process of polymerization of acrylic acid studied in this work is used for the production of dispersants. A specific average molecular weight with narrow distribution must be obtained to ensure the end-use product properties. The molecular weight must therefore be kept constant during the reaction. Set point values of MW are, therefore, specified according to the application of the polymeric product. The process under investigation actually produces a polymer with time-increasing molecular weights. Several experiments were carried out to validate the control strategy. Figure 21 shows a demonstration of the control strategy with a set point of 1,800 g/mol. The instantaneous molecular weight rapidly joins the desired molecular weight.

Figure 22 shows the flow rate of acrylic acid employed to control the molecular weight. Oscillations take place at the beginning of the reaction of the rapid change in the reaction rate, but later it is clear that a smooth flow is obtained.

Additional control results are displayed in Figure 23 where the M_n set point is 2,160 g/mol. Under feedback control, the process produces high molecular weights from the beginning of the reaction, which was not possible during open-loop operations. Figure 24 presents another validation of the control strategy with a molecular weight set point of 2,520 g/mol. In this case, it appears that the controller takes more time to produce such a high desired molecular weight. The delay in the

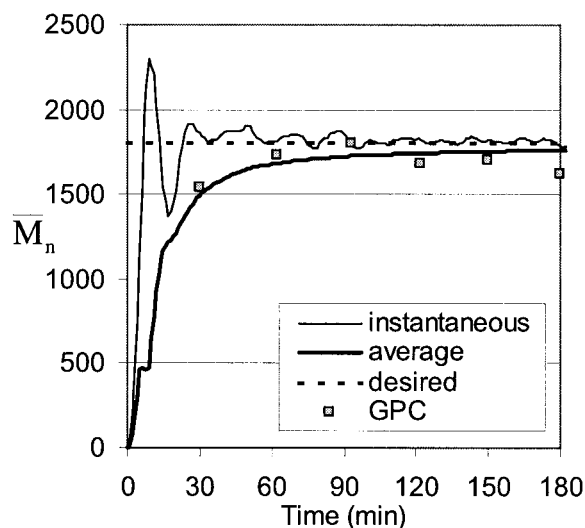


Figure 21. Control of \bar{M}_n , set point = 1,800 g/mol.

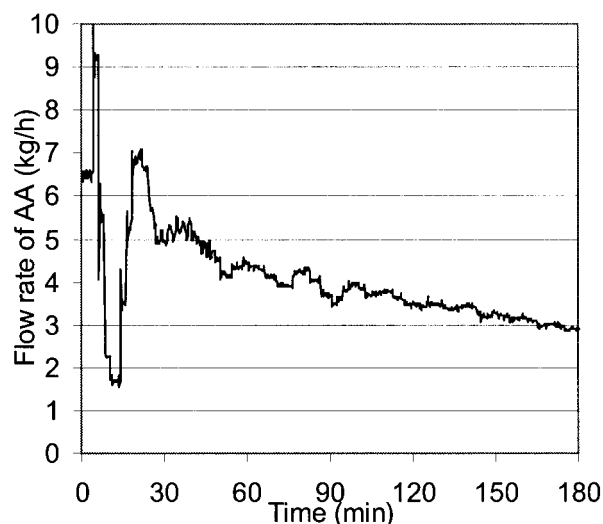


Figure 22. Flow rate of AA employed to control \bar{M}_n , desired $\bar{M}_n = 1,800$ g/mol.

convergence of M_n at the beginning of the reaction is because of the fact that its initial value lies far from the set point. The initial charge of the reactor does not contain any monomer. However, for security reasons, the reactor cannot be fed with monomer before the operation during the heating of the reactor. In order to accelerate the convergence of the controller for high molecular weights, the reactor should be charged with monomer at the beginning of the reaction, which requires further studies dealing with the operation safety. At present, in order to compensate for the lack of monomer, the controller feeds the reactor with the maximum allowed monomer flow rate at the beginning of the reaction, which disturbs the NIR measurements and the reaction kinetics. However, the instantaneous molecular weight stabilizes very quickly. A very slight detrimental effect on the accumulated molecular weight is observed.

Figure 25 presents the polydispersity index obtained during the polymerization operation performed with a desired M_n of

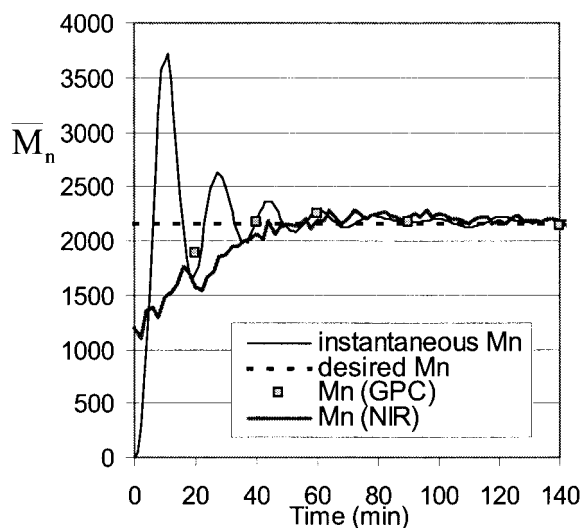


Figure 23. Control of \bar{M}_n , set point = 2160 g/mol.

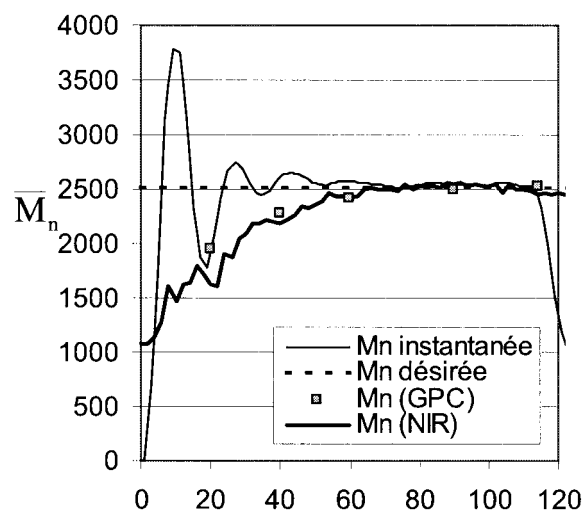


Figure 24. Control of \bar{M}_n , set point = 2500 g/mol.

2,520 g/mol. Controlling the molecular weight allows us to obtain a constant polydispersity index during the polymerization, whereas the same index was increasing with time during the original process, as shown in Figure 11, which is because of the fact that the polydispersity depends on the molecular weight.

Conclusion

Controlling the molecular-weight distribution is usually considered a difficult issue, because of the difficulty of measuring this variable on-line. In this work, NIR measurements were used to estimate the concentration of monomer and polymer in the reactor. A process model was established to correlate the evolution of the instantaneous molecular weight to the operating conditions, mainly the concentration of monomer, initiator, and solvent in the reactor. Nonlinear high gain observers were employed to identify the model parameters and the reaction rate. These observers offer the advantage of being easily tuned

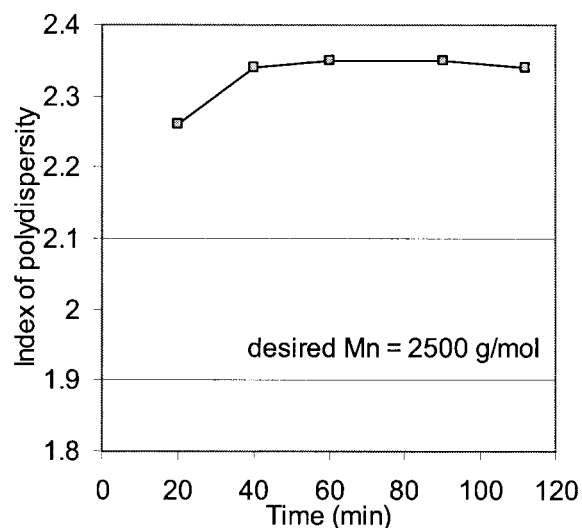


Figure 25. Polydispersity in the controlled experiment, desired $\bar{M} = 2,500$ g/mol.

and implemented. In order to estimate the ratio k_p/k_t , the reported observer uses the on-line NIR measurements if they are available. Interpolated off-line GPC measurements can also be used.

The control strategy uses a nonlinear geometric approach. This strategy allowed us to ensure the constant set point molecular weight by manipulating the inlet flow rate of monomer. Controlling the concentration of monomer permits the production of polymers with a constant molecular weight and polydispersity index during all the reaction, which is essential for many industrial applications.

The approach implemented here is applicable to solution polymerization reactors equipped with a NIR instrument, or any other instrument measuring the concentration of monomer and polymer in the reactor. However, few off-line GPC measurements of MW are also required. The controller was validated on a 30 L industrial pilot-scale reactor. Because the NIR calibration can be translated to bigger reactors, the measurements and control approach remain valid in larger scale processes.

Notation

D_p = degree of polymerization
 k_p = propagation rate constant, $\text{cm}^3/\text{mol/s}$
 k_f = transfer to solvent rate constant, $\text{cm}^3/\text{mol/s}$
 k_t = termination rate constant, $\text{cm}^3/\text{mol/s}$
 M_n = instantaneous number-average molecular weight of polymer, g/mol
 \bar{M}_n = cumulative number-average molecular weight of polymer, g/mol
 \bar{M}_w = cumulative weight-average molecular weight of polymer, g/mol
 MW_{AA} = molecular weight of AA, g/mol
 N_{AA} = number of moles of free monomer AA
 N_s = number of moles of solvent
 Q_{AA}^{in} = inlet molar flow rate of AA
 Q_i = inlet molar flow rate of initiator
 Q_s^{in} = inlet molar flow rate of solvent
 R_f = rate of transfer to solvent, mol/s
 R_p = propagation rate of monomer, mol/s
 R_t = termination rate, mol/s
 $[R^*]$ = concentration of radicals in the reactor, mol/cm^3
 V = volume of the reactor, cm^3

Greek letters

θ = a positive parameter regulating the rate of convergence of the observer
 κ_p = proportional gain of the PI controller
 τ_i = integral gain of the PI controller
 λ_i = i^{th} -order moment of the chain-length distribution of active chains
 μ_i = i^{th} -order moment of the chain-length distribution of inactive chains

Acknowledgment

The authors would like to thank the company Coatex for the financial support of the project.

Literature Cited

Adebekun, D., and F. J. Schork, "Continuous Solution Polymerization Reactor Control: 2. Estimation and Nonlinear Reference Control During

- Methyl Methacrylate Polymerization," *Ind. Eng. Chem. Res.*, **28**, 1846 (1989).
Aldridge, P. K., J. J. Kelly, and B. Callis, "Noninvasive Monitoring of Bulk Polymerization Using Short-Wavelength Near-Infrared Spectroscopy," *Analytical Chemistry*, **65**, 381 (1993).
Chabot P., L. Hedhli, and Ch. Olmstead, "On-line Monitoring of Emulsion Polymerization, AT-Process," *J. Proc. Analytical Chemistry*, **1**, 1 (2000).
Clay, P. A., and R. G. Gilbert, "Molecular Weight Distribution in Free-Radical Polymerization. I. Model Development and Implications for Data Interpretation," *Macromolecules*, **28**, 552 (1995).
Congalidis, J. P., J. R. Richards, and W. H. Ray, "Feedforward and Feedback Control of a Solution Copolymerization Reactor," *AIChE J.*, **35**, 891 (1989).
Crowley, T. J., and K. Y. Choi, "Experimental Studies on Optimal Molecular Weight Distribution Control in a Batch-Free Radical Polymerization Process," *Chem. Eng. Sci.*, **53** (15), 2769 (1998).
Dimitratos, J., C. Georgakakis, M. S. El-Aasser, and A. Klein, "Dynamic Modeling and State Estimation of an Emulsion Copolymerization Reactor," *Comp. Chem. Eng.*, **13**, 21 (1989).
Echevarria, A., J. R. Leiza, J. C. de la Cal, and J. M. Asua, "Molecular-Weight Distribution Control in Emulsion Polymerization," *AIChE J.*, **44**(7), 1667 (1998).
Ellis, M. F., T. W. Taylor, and K. F. Jensen, "On-line Molecular Weight Distribution Estimation and Control in Batch Polymerization," *AIChE J.*, **40**(3), 445 (1994).
Farza, M., H. Hammouri, S. Othman, and K. Busawon, "Nonlinear Observers for Parameter Estimation in Bioprocesses," *Chem. Eng. Sci.*, **52**(23), 4251 (1997).
Florenzano, F. H., R. Strelitzki, and W. F. Reed, "Absolute On-Line Monitoring of Molar Mass During Polymerization Reactions," *Macromolecules*, **31**, 7226 (1998).
Ghielmi, A., G. Storti, and M. Morbidelli, "Molecular Weight Distribution in Emulsion Polymerization: Role of Active Chain Compartmentalization," *Macromolecules*, **31**, 7172 (1998).
Gossen, P. D., J. F. MacGregor, and R. H. Pelton, "Composition and Particle Diameter for Styrene/Methyl Methacrylate Copolymer Latex using UV and NIR Spectroscopy," *Appl. Spectroscopy*, **47**, 11 (1993).
Kabanov, V. A., D. A. Topchiev, and T. M. Karaputadze, "Some Features of Radical Polymerization of Acrylic and Methacrylic Acid Salts in Aqueous Solutions," *J. Poly. Sci., Symp.*, **42**, 173 (1973).
Kozub, D. J., and J. F. MacGregor, "Feedback Control of Polymer Quality in Semi-Batch Copolymerization Reactors," *Chem. Eng. Sci.*, **47**, 942 (1992).
Long T. E., H. Y. Liu, B. A. Schell, D. M. Teegarden and D. S. Uerz, "Determining of Solution Kinetics by NIR Infrared Spectroscopy. 1. Living Anionic Polymerization Processes," *Macromolecules*, **26**, 6237 (1993).
Louie, B. M., and D. S. Soong, "Optimization of Batch Polymerization Processes- Narrowing the MWD. I. Model Simulation," *J. Appl. Pol. Sci.*, **30**, 3707 (1985).
Martin, J. R., J. F. Johnson, and A. R. Cooper, "Mechanical Properties of Polymers: The Influence of Molecular Weight and Molecular Weight Distribution," *J. Macromol. Sci. Rev. Macromol. Chem.*, **C8**, 57 (1972).
Santos, A. F., E. L. Lima, and J. C. Pinto, "In-line Evaluation of Average Particle Size in Styrene Suspension Polymerizations Using Near-Infrared Spectroscopy," *J. Appl. Poly. Sci.*, **70**, 1737 (1998).
Santos, A. S., E. L. Lima, J. C. Pinto, "Control and Design of Average Particle Size in Styrene Suspension Polymerizations Using NIRS," *J. Appl. Poly. Sci.*, **77**, 453 (2000).

Manuscript received Dec 20, 2002, and revision received July 8, 2003.